

# Probing neutrino-nucleus interaction in DUNE and MicroBooNE

R K Pradhan <sup>a,1</sup>, R Lalnuntluanga <sup>b,1</sup>, and A Giri <sup>c,1</sup>

<sup>1</sup>*Department of Physics, Indian Institute of Technology Hyderabad, Hyderabad, 502284, Telangana, India*

**Abstract:** The neutrino experiments utilize heavy nuclear targets to achieve high statistics neutrino-nucleus interaction event rate, which leads to systematic uncertainties in the oscillation parameters due to the nuclear effects and uncertainties in the cross-section. Understanding the interaction of neutrinos with the nucleus becomes crucial in determining the oscillation parameters with high precision. We investigate the uncertainty in quasi-elastic interaction due to nuclear effects by selecting exactly 1 proton, 0 pions, and any number of neutrons in the final state using DUNE and MicroBooNE detectors, and the effects on oscillation parameters in the DUNE detector. The kinematic method along with this selection can be used for accurate neutrino energy reconstruction in the quasi-elastic channel where the nuclear effects are inevitable.

## 1 Introduction

The primary goal of the current and future neutrino experiments is precisely measuring the neutrino oscillation parameters. The oscillation probability depends on the neutrino energy and the neutrino beam is not mono-energetic, it spreads in a broad range of energy spectrum due to their production in the decay of produced hadrons. So, an event-by-event neutrino energy reconstruction is required for a better understanding of uncertainty in neutrino oscillation. Due to high statistics requirements, neutrino experiments use heavy nuclear targets (Argon [1, 2], Iron [3, 4], Water [5], Oxygen [6], etc), which arises complications in the reconstruction due to the complexity of the nucleus. For accurate neutrino energy reconstruction, understanding neutrino-nucleus interactions is very crucial.

<sup>a</sup>[kumarriteshpradhan@gmail.com](mailto:kumarriteshpradhan@gmail.com)

<sup>b</sup>[tluangaralte.phy@gmail.com](mailto:tluangaralte.phy@gmail.com)

<sup>c</sup>[giria@phy.iith.ac.in](mailto:giria@phy.iith.ac.in)

Most Long-Baseline Neutrino Experiments (LBNE) run in the few GeV energy regions where quasi-elastic scattering is one of the most important interaction channels however there is a significant contribution of 2p-2h interaction which makes the situation complicated [7, 8]. In this work, we focus on muon neutrino charge current quasi-elastic (CCQE) scattering ( $\nu_\mu n \rightarrow \mu^- p$ ). In a nucleus, the neutron is neither free nor at rest, but it moves and is bound inside a nuclear potential. To understand CCQE scattering, one can refer to impulse approximation (IA) [9], in which interactions occur on the individual nucleons. In the IA, the neutrino interacts with a pair of nucleon inside the nucleus, or a bound nucleon followed by the final state interaction (FSI) [10]. Due to FSI, the proton produced in primary interaction undergoes various hadronic scattering such as (in)elastic scattering, pion production, hadron absorption, and charge exchange which results in knocked-out nucleons and mesons in the final state. This results in the misidentification of non-QE events as QE events. Pion production is the major background to the QE scattering events. In some events, these produced pions again get absorbed leading to two nucleon knock-out, called 2p-2h scattering. The cross-section of CCQE-like interactions measured in T2K can be explored in Ref. [11]. Due to FSI, a CCQE can also produce pion, thus can't be classified as CCQE-like. These backgrounds lead to an uncertainty in the neutrino energy reconstruction, which impacts the oscillation parameters. The effects on the parameters of oscillation for experiments such as T2K and MiniBooNE are studied here [12, 13].

Monte Carlo event generators are used for the simulations of neutrino interactions, developed with different nuclear models. They are used for predictions and improvement of the experiments. The generators such as GENIE [14], NuWro [15], GiBUU [16], and NEUT [17] are extensively used for physics analysis. In this work, we aim to select high-purity CCQE events for DUNE detectors [18] using the realistic particle thresholds, and its effects on the os-

cillation parameters is studied using both GENIE and NuWro. Previous studies for LBNE using the GiBUU model can be found in Ref. [19]. The analysis methods for our event selection have been implemented for the MicroBooNE detector [20] using GENIE and NuWro models.

This paper is organized as follows. In section 2, we present the formalism for the neutrino interactions with the nuclear target and the methods for reconstructing the energy of the neutrino. The Monte Carlo event generators are described in section 3. The simulation specifications of the DUNE and MicroBooNE detectors are mentioned in section 4. We then discuss the results from our analysis in section 5, followed by the conclusion in section 6.

## 2 Formalism

Consider a charged current neutrino interaction with a nuclear target knocking out  $n$  nucleons and producing  $m$  mesons. These produced particles can be used for the neutrino energy reconstruction, using the kinematic and calorimetric methods [21]. The reconstructed energy from the generalized kinematic approach [21] is,

$$E_\nu = \frac{2(nM - \varepsilon_n)E_l + W^2 - (nM - \varepsilon_n)^2 - m_l^2}{2(nM - \varepsilon_n - E_l + |k_l|\cos\theta)} \quad (1)$$

The invariant hadronic mass squared is defined as,

$$W^2 = \left( \sum_i E_{p'_i} + \sum_j E_{h'_j} \right)^2 - \left( \sum_i p'_i + \sum_j h'_j \right)^2$$

where,  $E_{p'}$  and  $p'$  ( $E_{h'}$  and  $h'$ ) are the energy, and momentum of final state nucleons (mesons) respectively.  $M$  ( $m_l$ ) is the mass of the final state nucleon (lepton),  $E_l$  and  $k_l$  are the energy and momentum of the outgoing lepton respectively, and  $\theta$  is the scattering angle,  $\varepsilon_n$  the neutron separation energy.

For a pure charge current quasi-elastic (CCQE) scattering, where the hit nucleon (neutron) is at rest, the kinematic method for reconstructing the neutrino energy [13],

$$E_\nu = \frac{2(M_n - E_B)E_l - (E_B^2 - 2M_n E_B + m_l^2 + \Delta M^2)}{2(M_n - E_B - E_l + |k_l|\cos\theta)} \quad (2)$$

where,  $M_n$  is the free neutron rest mass,  $\Delta M^2 = M_n^2 - M_p^2$ ,  $M_p$  is the rest mass of the proton, and  $E_B$  the binding energy.

For better accuracy in the analysis, rather than assuming constant binding energy value, we consider a distribution for the neutron excitation energy for the nucleus [22], for both  $^{12}\text{C}$  and  $^{40}\text{Ar}$  target. A Gaussian distribution of separation energy  $E$  with mean  $E_\alpha$ , and deviation  $\sigma_\alpha$ , is considered according to table 1 for  $^{12}\text{C}$  [23], and in table 2 for  $^{40}\text{Ar}$  [24].

| Subshell   | $E_\alpha$ (MeV) | $\sigma_\alpha$ (MeV) | No. neutron $n_\alpha$ |
|------------|------------------|-----------------------|------------------------|
| $1s_{1/2}$ | 40.8             | 9.1                   | 2                      |
| $1p_{3/2}$ | 20.3             | 5                     | 4                      |

**Table 1** Neutron Shell Structure in  $^{12}\text{C}$  [23]

| Subshell   | $E_\alpha$ (MeV) | $\sigma_\alpha$ (MeV) | No. neutron $n_\alpha$ |
|------------|------------------|-----------------------|------------------------|
| $1s_{1/2}$ | 62               | 6.25                  | 2                      |
| $1p_{3/2}$ | 40               | 3.75                  | 4                      |
| $1p_{1/2}$ | 35               | 3.75                  | 2                      |
| $1d_{5/2}$ | 18               | 1.25                  | 6                      |
| $2s_{1/2}$ | 13.15            | 1                     | 2                      |
| $1d_{3/2}$ | 11.45            | 0.75                  | 4                      |
| $1f_{7/2}$ | 5.56             | 0.75                  | 2                      |

**Table 2** Neutron Shell Structure in  $^{40}\text{Ar}$  [24]

The probability distribution for the separation energy is given by,

$$P(E) = \frac{1}{N} \sum_\alpha n_\alpha G(E - E_\alpha, \sigma_\alpha) \quad (3)$$

where the sum of neutrons

$$N = \sum_\alpha n_\alpha$$

and  $G(E - E_\alpha, \sigma_\alpha)$  is the distribution function.

For oscillation analysis, the survival probability of muon neutrino can be calculated by using the following expression [25],

$$P_{\nu_\mu \rightarrow \nu_\mu} \approx 1 - \sin^2 2\theta_{\mu\mu} \sin^2 \frac{\Delta m_{\mu\mu}^2 L}{4E_\nu} \quad (4)$$

with

$$\sin^2 \theta_{\mu\mu} = \cos^2 \theta_{13} \sin^2 \theta_{23}$$

$$\Delta m_{\mu\mu}^2 = \sin^2 \theta_{12} \Delta m_{31}^2 + \cos^2 \theta_{12} \Delta m_{32}^2 + \cos \delta_{CP} \sin \theta_{13} \sin 2\theta_{12} \tan \theta_{23} \Delta m_{21}^2$$

The values of the oscillation parameters,  $\Delta m^2$  and  $\theta$  are taken from Ref. [26]. The distance of the DUNE far detector is  $L \approx 1300$  km far from the near detector.

## 3 Monte Carlo Event Generator

In this work, two MC generators, GENIE and NuWro are used for simulating the neutrino-nucleus interactions. Both GENIE and NuWro are used by accelerator-based neutrino experiments. The Fermi Gas Model [27] is implemented to define the impact of the nuclear environment considering nucleon-nucleon correlation effects [28] in GENIE, and the spectral function [29] in NuWro.

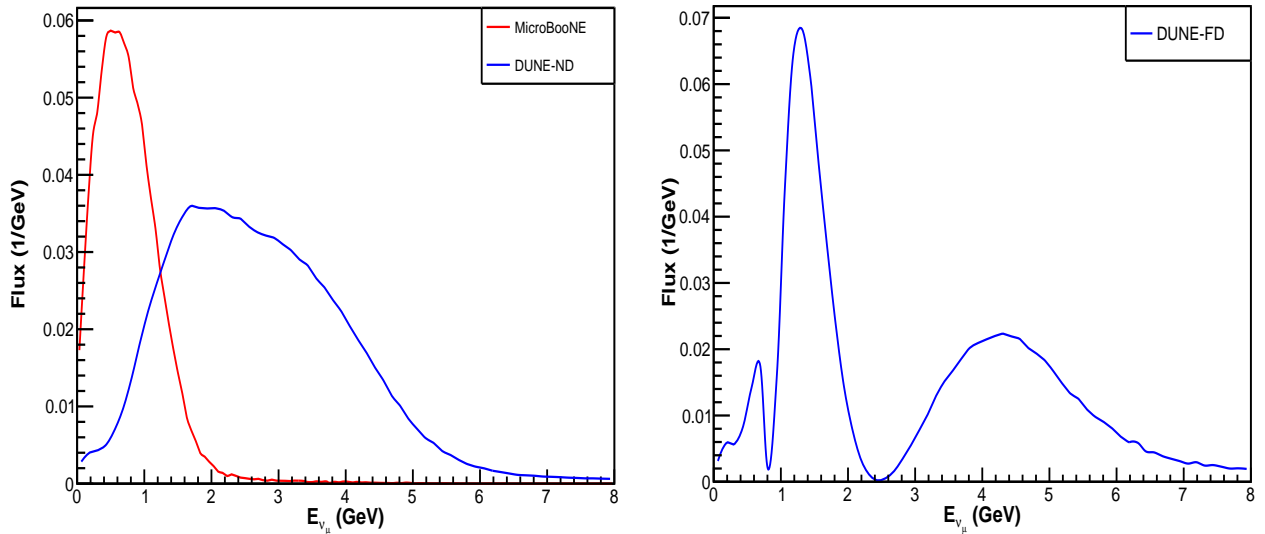


**Fig. 1** Unoscillated muon neutrino flux for DUNE Near detector and MicroBooNE (left) and oscillated flux for DUNE Far detector (right).

The default model for QE scattering in GENIE is the Llewellyn-Smith (LS) model [30]. The new models for QE scattering and MEC/2p-2h processes in GENIE are the Valencia QE model [31, 32] and SuSAv2 [33, 34]. The Valencia model is based on the Local Fermi Gas model with Coulomb correction effects and Random Phase Approximation (RPA). In contrast, the SuSAv2 is based on the Relativistic Mean Field (RMF) theory. In NuWro, the QE interactions are described by the LS model with options for vector and dipole axial vector form factors. GENIE implements the axial mass  $M_A$  extending from 0.99 to 1.2  $\text{GeV}/c^2$ , whereas NuWro confines this parameter in a range of 0.94-1.03  $\text{GeV}/c^2$ . In this work, the value of the CCQE axial mass is considered as  $\approx 0.96 \text{ GeV}/c^2$  in both GENIE and NuWro, and the vector form factors used are BBA07 [35] and BBA05 [36] respectively. GENIE has 4 FSI models: hA, hN, INCL++, and Geant4 [37], while in NuWro, the FSI is described by the cascade model based on the algorithm by Metropolis *et al.* [38]. Empirical MEC model [39] is also available for MEC/2p-2h scattering in GENIE, and transverse enhancement model [40] and Marteau-Martini model [8] are also available in NuWro for 2p-2h scattering.

The baryonic resonances are modeled using the Berger-Sehgal (BS) model [41] in GENIE. NuWro uses the Rein-Sehgal (RS) model [42] for  $\Delta(1232)$  resonance, and the Adler-Rarita-Schwinger model [43] for higher resonances. Other available resonance models in GENIE are Kuzmin-Lyubushkin-Naumov (KLN) [44] and the RS model.

In the inelastic region (DIS), both the generators use the Bodek-Yang Model [45] for the cross-section calculation, and utilize PYTHIA [46] to produce hadronic final states with different values of PYTHIA parameters such as invari-

ant hadronic mass  $W$ . GENIE employs it to  $W = 1.8$  or  $2.0$  GeV with KNO scaling [47] while NuWro is to 1.6 GeV. The invariant hadronic mass threshold used in this work is  $W = 1.9$  GeV in GENIE and 1.6 GeV in NuWro.

#### 4 Simulation Details

In this paper, nuclear effects on energy reconstruction are analyzed for the DUNE near and far detector and the MicroBooNE detector. DUNE mainly uses Argon as the target material. The proposed DUNE near detector HpgTPC [48] consists of Argon and Methane ( $\text{CH}_4$ ), and liquid Argon as the target material in the far detector. MicroBooNE also uses liquid Argon targets. CC  $\nu_\mu$  interaction are simulated for Argon and Carbon target using the DUNE [49] and MicroBooNE  $\nu_\mu$  flux [50] as shown in Fig. 1. The GENIE v3.01.00 (tune G18\_10a\_02\_11a) and NuWro-21.09.2 are used for the simulation. We consider realistic simulations and include the Quasi-elastic (QE), Meson exchange (MEC/2p-2h), Resonance (RES), and Deep Inelastic Scattering (DIS) in neutrino mode. In the RES channel, we consider only the first resonance region,  $\Delta$  or  $P_{33}(1232)$ . For the simulation, we have used the Nieves model for QE, the Berger Sehgal model for the resonance, and the CCQE axis mass ( $M_A$ ) is considered to be  $0.96 \text{ GeV}/c^2$ . For FSI, the hA model is employed in GENIE, and the Oset model in NuWro. To study the FSI effect, we have also simulated the interaction events by switching ON/OFF the FSI in both MC generators.

Ideally, CCQE interaction can be identified as 1 proton and 0 pions in the final state. But it could be possible that

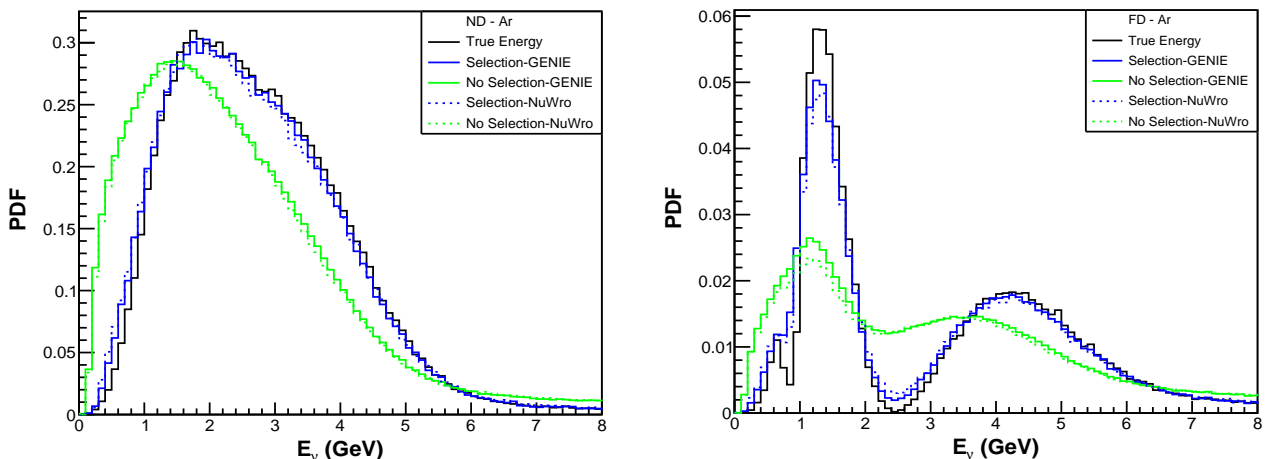


**Fig. 2** The probability density function (PDF) of reconstructed neutrino energy for Argon in DUNE near (left) and far (right) detector using GENIE (solid) and NuWro (dotted).

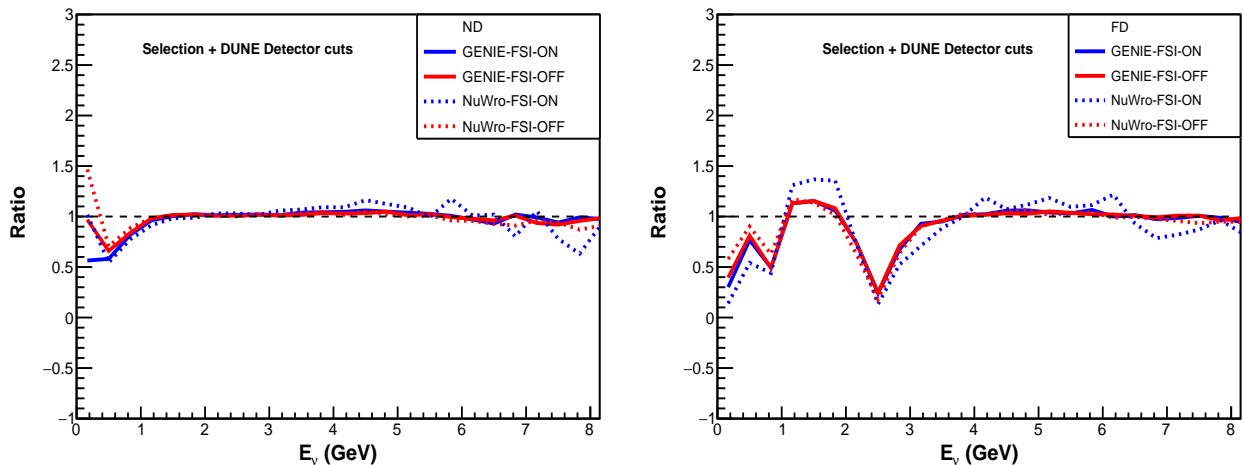


**Fig. 3** The ratio of true and reconstructed energy PDF as a function of neutrino energy for Argon in DUNE near (left) and far (right) detectors with FSI (blue) and without FSI (red) using GENIE (solid) and NuWro (dotted).

the pion produced due to FSI gets absorbed inside the nucleus knocking out nucleons. We consider a selection of exactly 1 proton, 0 pions, and any number of neutrons in the final state [19] for the CCQE interaction. The unobserved neutrons in the detector are a consequence of the nuclear effects. Due to limitations in the sensitivity of detectors, all the produced particles cannot be detected. We have applied the detector cuts for both the near and far detectors. The detection thresholds for the DUNE ND are, the total energy cut for muon is 226 MeV [51] ( $\approx 200$  MeV momentum), and a minimum kinetic energy threshold of 3 MeV for proton [52]. The neutrons in the detector have a threshold of kinetic energy from 50 MeV to 700 MeV [51]. In case of FD, muons have a detector threshold of 30 MeV kinetic energy, and 50 MeV for protons and neutrons [18]. A study

on the proton kinetic energy threshold of 20 MeV with 80% efficiency can be found in Ref. [53]. In the MicroBooNE detector, the leading proton has a threshold momentum of 300 MeV/c ( $\approx 47$  MeV kinetic energy), and the momentum threshold for muon is 100 MeV/c [50]. The selection (1 proton + 0 pions + X neutrons) with the corresponding detector thresholds for the DUNE and MicroBooNE detectors are applied to reconstruct the neutrino energy for the CCQE.

## 5 Results

The event distributions of neutrino energy for Argon in both ND and FD are shown in Fig. 2. For the ND, the reconstructed energy using the kinematic method (green) is shifted by  $\approx 0.4$  GeV towards lower energies, compared to

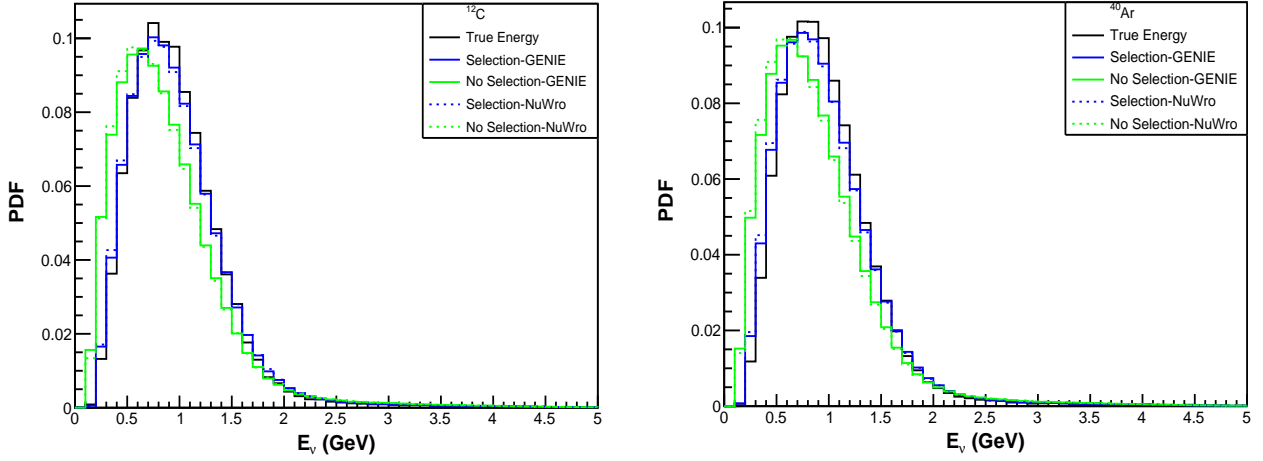


**Fig. 4** The PDF of reconstructed neutrino energy for Carbon (left) and Argon (right) in MicroBooNE detector using GENIE (solid) and NuWro (dotted).

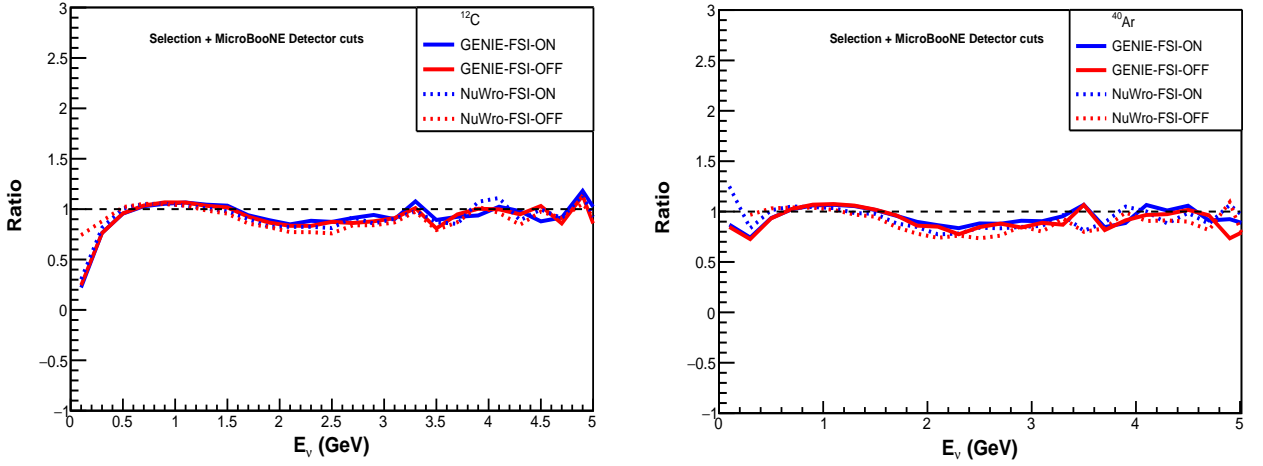


**Fig. 5** The PDF ratio of true and reconstructed energy as a function of neutrino energy for Carbon (left) and Argon (right) in MicroBooNE detectors with FSI (blue) and without FSI (red) using GENIE (solid) and NuWro (dotted).

the true energy distribution (black). The distribution at FD after oscillation is given on the right panel (Fig. 2). It can be observed clearly that without the selection, the distribution is distorted with flattening of the minima around 2.4 GeV. The event rate is significantly low at the second maxima at 1.4 GeV. When the selection (1 proton + 0 pions + X neutrons) is considered along with the DUNE ND and FD detector cuts, the reconstructed energy distribution (blue) agrees with the true energy for both ND and FD. The shift of reconstructed energy is reduced to less than 100 MeV compared to true neutrino energy. The results using GENIE are represented as solid lines. Similarly, NuWro (dotted) results show the same effects as GENIE. For evaluating the uncertainty in the reconstruction, we consider the event ratio distribution of true energy with the reconstructed energy which is shown in

Fig.3. To further quantify the effect of FSI, we consider the ratio with FSI and without FSI. For the ND, the ratio is close to 1 but in the lower energy region ( $< 1$  GeV), the reconstructed energy differs from the true energy due to nuclear effects. As a result of the nuclear effects, 91 % of events are true CCQE, and the remaining events are mostly contributed by 2p-2h and DIS, out of the selected events. In the context of far detector, the reconstructed energy disagrees with the true energy in the maxima and minima regions as there is a downward shift in the reconstructed events. When the FSI is switched off, it can be seen that the ratio is closer to unity in the lower energy range, which indicates that the effect of the FSI contributes to the uncertainty in the reconstruction. The probability distribution of neutrino energy for Carbon and Argon in the MicroBooNE detector is given in Fig. 4.

There is a shift of  $\approx 0.2$  GeV in the reconstructed energy without the selection i.e. the kinematic method. However, the reconstructed energy agrees with true energy when the selection along with detector thresholds are considered. Out of the selected events, 96% of events are from true CCQE contributions. From the ratio of true neutrino energy to reconstructed energy in Fig. 5, the selection criteria can be considered to significantly identify the CCQE interaction, and the uncertainty could be due to the impact of final state interactions.

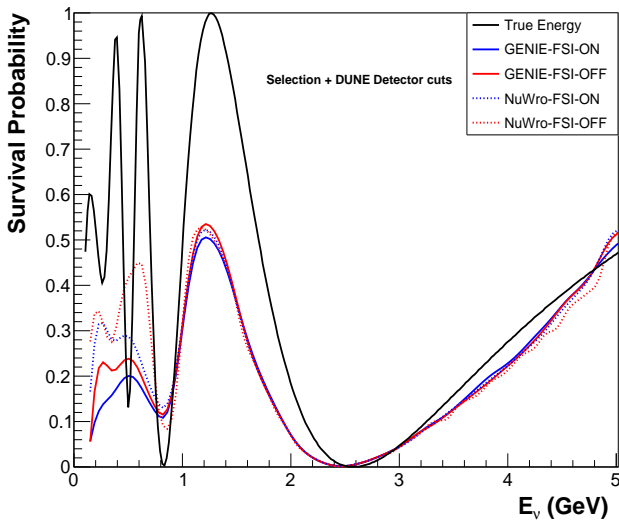


**Fig. 6** The muon neutrino survival probability in DUNE as a function of true energy without any selection (black) and the reconstructed energy for QE with FSI (blue) and without FSI (red) using GENIE (solid) and NuWro (dotted) considering the selection with detector cuts.

The effects on the neutrino oscillation parameters using the selection (1 proton + 0 pions + X neutrons) are studied. The survival probability of muon neutrinos is shown in Fig. 6. The true survival probability is calculated using equation 4, and the same parameters are used from [26] as a function of true neutrino energy. Assuming the experimental analysis, the survival probability is calculated by taking the ratio of oscillated (FD) and unoscillated (ND) event distributions. In Fig. 6, the black curve shows the survival probability as a function of true energy, the blue curve represents the survival probability as a function of the reconstructed energy by considering the selection with detector cuts and the FSI effects, and without the FSI is shown by the red curve. We can observe that there is a significant influence in the absolute values, both at the first maximum and first minimum, while the positions of maximum and minimum are less affected when we consider the selections. One can see the effect of FSI in the lower energy range and at the first maxima. This indicates a notable discrepancy in the mixing angle, while

the impact on  $\Delta m^2$  is comparatively negligible. The same effect has been observed for T2K by Coloma et al. [54] as well.

## 6 Conclusion

The purity of QE interactions selection for the Micro-BooNE detector, and the DUNE near and far detectors and their effect on oscillation parameters has been studied using the Monte Carlo neutrino event generators GENIE and NuWro. The physics potential studies on LBNE have shown that an energy resolution of 100 MeV is required to differentiate between different physics properties [55]. The selection of 1 proton, 0 pions, and X neutrons for CCQE shows a weighty discrepancy between the reconstructed and the true neutrino energy approximately by 100 MeV which is the required resolution. This shift of around 100 MeV is observed in both the ND and FD for both generators. The uncertainty in reconstruction due to the nuclear effects notably affects the mixing angle, with comparatively lesser effects on  $\Delta m^2$ . Also, the ratio of true and reconstructed energy distribution in the high-energy regions indicates the viability of this method in higher-energy experiments.

## Acknowledgements

R K Pradhan acknowledges the DST-INSPIRE grant (2022/IF220293) for financial support. R Lalnuntluanga thanked the Council of Scientific & Industrial Research (file number: 09/1001(0054)/2019-EMR-I) for the financial grant. R Lalnuntluanga and A Giri credited the grant support of the Department of Science and Technology (SR/MF/PS-01/2016-IITH/G).

## References

1. Anderson C, et al. First Measurements of Inclusive Muon Neutrino Charged Current Differential Cross Sections on Argon. *Phys Rev Lett.* 2012;108:161802. <https://doi.org/10.1103/PhysRevLett.108.161802>. [arXiv:1111.0103](https://arxiv.org/abs/1111.0103). [hep-ex].
2. Acciarri R, et al. Measurements of Inclusive Muon Neutrino and Antineutrino Charged Current Differential Cross Sections on Argon in the NuMI Antineutrino Beam. *Phys Rev D.* 2014;89(11):112003. <https://doi.org/10.1103/PhysRevD.89.112003>. [arXiv:1404.4809](https://arxiv.org/abs/1404.4809). [hep-ex].
3. Abe K, et al. Measurement of the inclusive  $\nu_\mu$  charged current cross section on iron and hydrocarbon in the T2K on-axis neutrino beam. *Phys Rev D.* 2014;90(5):052010. <https://doi.org/10.1103/PhysRevD.90.052010>. [arXiv:1407.4256](https://arxiv.org/abs/1407.4256). [hep-ex].

4. Tice BG, et al. Measurement of Ratios of  $\nu_\mu$  Charged-Current Cross Sections on C, Fe, and Pb to CH at Neutrino Energies 2-20 GeV. *Phys Rev Lett.* 2014;112(23):231801. <https://doi.org/10.1103/PhysRevLett.112.231801>. [arXiv:1403.2103](https://arxiv.org/abs/1403.2103). [hep-ex].
5. Abe K, et al. First measurement of the muon neutrino charged current single pion production cross section on water with the T2K near detector. *Phys Rev D.* 2017;95(1):012010. <https://doi.org/10.1103/PhysRevD.95.012010>. [arXiv:1605.07964](https://arxiv.org/abs/1605.07964). [hep-ex].
6. Abe K, et al. Measurement of the neutrino-oxygen neutral-current interaction cross section by observing nuclear deexcitation  $\gamma$  rays. *Phys Rev D.* 2014;90(7):072012. <https://doi.org/10.1103/PhysRevD.90.072012>. [arXiv:1403.3140](https://arxiv.org/abs/1403.3140). [hep-ex].
7. Aguilar-Arevalo AA, et al. First Measurement of the Muon Neutrino Charged Current Quasielastic Double Differential Cross Section. *Phys Rev D.* 2010;81:092005. <https://doi.org/10.1103/PhysRevD.81.092005>. [arXiv:1002.2680](https://arxiv.org/abs/1002.2680). [hep-ex].
8. Martini M, Ericson M, Chanfray G, Marteau J. A Unified approach for nucleon knock-out, coherent and incoherent pion production in neutrino interactions with nuclei. *Phys Rev C.* 2009;80:065501. <https://doi.org/10.1103/PhysRevC.80.065501>. [arXiv:0910.2622](https://arxiv.org/abs/0910.2622). [nucl-th].
9. Benhar O, Farina N, Nakamura H, Sakuda M, Seki R. Electron- and neutrino-nucleus scattering in the impulse approximation regime. *Phys Rev D.* 2005;72:053005. <https://doi.org/10.1103/PhysRevD.72.053005>. [arXiv:hep-ph/0506116](https://arxiv.org/abs/hep-ph/0506116).
10. Dytman S. Final state interactions in neutrino-nucleus experiments. *Acta Phys Polon B.* 2009;40:2445–2460.
11. Abe K, et al. Measurement of double-differential muon neutrino charged-current interactions on  $C_8H_8$  without pions in the final state using the T2K off-axis beam. *Phys Rev D.* 2016;93(11):112012. <https://doi.org/10.1103/PhysRevD.93.112012>. [arXiv:1602.03652](https://arxiv.org/abs/1602.03652). [hep-ex].
12. Lalakulich O, Mosel U, Gallmeister K. Energy reconstruction in quasielastic scattering in the Mini-BooNE and T2K experiments. *Phys Rev C.* 2012;86:054606. <https://doi.org/10.1103/PhysRevC.86.054606>. [arXiv:1208.3678](https://arxiv.org/abs/1208.3678). [nucl-th].
13. Coloma P, Huber P, Jen CM, Mariani C. Neutrino-nucleus interaction models and their impact on oscillation analyses. *Phys Rev D.* 2014;89(7):073015. <https://doi.org/10.1103/PhysRevD.89.073015>. [arXiv:1311.4506](https://arxiv.org/abs/1311.4506). [hep-ph].
14. Andreopoulos C, et al. The GENIE Neutrino Monte Carlo Generator. *Nucl Instrum Meth A.* 2010;614:87–104. <https://doi.org/10.1016/j.nima.2009.12.009>. [arXiv:0905.2517](https://arxiv.org/abs/0905.2517). [hep-ph].
15. Juszczak C, Nowak JA, Sobczyk JT. Simulations from a new neutrino event generator. *Nucl Phys B Proc Suppl.* 2006;159:211–216. <https://doi.org/10.1016/j.nuclphysbps.2006.08.069>. [arXiv:hep-ph/0512365](https://arxiv.org/abs/hep-ph/0512365).
16. Buss O, Gaitanos T, Gallmeister K, van Hees H, Kaskulov M, Lalakulich O, et al. Transport-theoretical Description of Nuclear Reactions. *Phys Rept.* 2012;512:1–124. <https://doi.org/10.1016/j.physrep.2011.12.001>. [arXiv:1106.1344](https://arxiv.org/abs/1106.1344). [hep-ph].
17. Hayato Y, Pickering L. The NEUT neutrino interaction simulation program library. *Eur Phys J ST.* 2021;230(24):4469–4481. <https://doi.org/10.1140/epjst/s11734-021-00287-7>. [arXiv:2106.15809](https://arxiv.org/abs/2106.15809). [hep-ph].
18. Acciarri R, et al. Long-Baseline Neutrino Facility (LBNF) and Deep Underground Neutrino Experiment (DUNE): Conceptual Design Report, Volume 4 The DUNE Detectors at LBNF. 2016 1; [arXiv:1601.02984](https://arxiv.org/abs/1601.02984). [physics.ins-det].
19. Mosel U, Lalakulich O, Gallmeister K. Energy reconstruction in the Long-Baseline Neutrino Experiment. *Phys Rev Lett.* 2014;112:151802. <https://doi.org/10.1103/PhysRevLett.112.151802>. [arXiv:1311.7288](https://arxiv.org/abs/1311.7288). [nucl-th].
20. Acciarri R, et al. Design and Construction of the MicroBooNE Detector. *JINST.* 2017;12(02):P02017. <https://doi.org/10.1088/1748-0221/12/02/P02017>. [arXiv:1612.05824](https://arxiv.org/abs/1612.05824). [physics.ins-det].
21. Ankowski AM, Benhar O, Coloma P, Huber P, Jen CM, Mariani C, et al. Comparison of the calorimetric and kinematic methods of neutrino energy reconstruction in disappearance experiments. *Phys Rev D.* 2015;92(7):073014. <https://doi.org/10.1103/PhysRevD.92.073014>. [arXiv:1507.08560](https://arxiv.org/abs/1507.08560). [hep-ph].
22. Furmanski AP, Sobczyk JT. Neutrino energy reconstruction from one muon and one proton events. *Phys Rev C.* 2017;95(6):065501. <https://doi.org/10.1103/PhysRevC.95.065501>. [arXiv:1609.03530](https://arxiv.org/abs/1609.03530). [hep-ex].
23. Frullani S, Mougey J. Single Particle Properties of Nuclei Through  $(e, e' p)$  Reactions. *Adv Nucl Phys.* 1984;14:1–283.
24. Ankowski AM, Sobczyk JT. Construction of spectral functions for medium-mass nuclei. *Phys Rev C.* 2008;77:044311. <https://doi.org/10.1103/PhysRevC.77.044311>. [arXiv:0711.2031](https://arxiv.org/abs/0711.2031). [nucl-th].
25. Zyla PA, et al. Review of Particle Physics. *PTEP.* 2020;2020(8):083C01. <https://doi.org/10.1093/ptep/ptaa104>.
26. Bishai M, Diwan MV, Kettell S, Stewart J, Viren B, Worchester E, et al. Neutrino Oscillations in the Precision Era. 2012 3; [arXiv:1203.4090](https://arxiv.org/abs/1203.4090). [hep-ex].
27. Bodek A, Ritchie JL. Further Studies of Fermi Motion Effects in Lepton Scattering from Nuclear Targets. *Phys Rev D.* 1981;24:1400. <https://doi.org/10.1103/>

- [PhysRevD.24.1400](#).
28. Bodek A, Ritchie JL. Fermi Motion Effects in Deep Inelastic Lepton Scattering from Nuclear Targets. *Phys Rev D*. 1981;23:1070. <https://doi.org/10.1103/PhysRevD.23.1070>.
  29. Benhar O, Fabrocini A, Fantoni S. The Nucleon Spectral Function in Nuclear Matter. *Nucl Phys A*. 1989;505:267–299. [https://doi.org/10.1016/0375-9474\(89\)90374-6](https://doi.org/10.1016/0375-9474(89)90374-6).
  30. Llewellyn Smith CH. Neutrino Reactions at Accelerator Energies. *Phys Rept*. 1972;3:261–379. [https://doi.org/10.1016/0370-1573\(72\)90010-5](https://doi.org/10.1016/0370-1573(72)90010-5).
  31. Nieves J, Amaro JE, Valverde M. Inclusive quasi-elastic neutrino reactions. *Phys Rev C*. 2004;70:055503. [Erratum: *Phys.Rev.C* 72, 019902 (2005)]. <https://doi.org/10.1103/PhysRevC.70.055503>. [arXiv:nucl-th/0408005](https://arxiv.org/abs/nucl-th/0408005).
  32. Gran R, Nieves J, Sanchez F, Vicente Vacas MJ. Neutrino-nucleus quasi-elastic and 2p2h interactions up to 10 GeV. *Phys Rev D*. 2013;88(11):113007. <https://doi.org/10.1103/PhysRevD.88.113007>. [arXiv:1307.8105](https://arxiv.org/abs/1307.8105). [hep-ph].
  33. Dolan S, Megias GD, Bolognesi S. Implementation of the SuSAv2-meson exchange current 1p1h and 2p2h models in GENIE and analysis of nuclear effects in T2K measurements. *Phys Rev D*. 2020;101(3):033003. <https://doi.org/10.1103/PhysRevD.101.033003>. [arXiv:1905.08556](https://arxiv.org/abs/1905.08556). [hep-ex].
  34. Megias GD, Amaro JE, Barbaro MB, Caballero JA, Donnelly TW, Ruiz Simo I. Charged-current neutrino-nucleus reactions within the superscaling meson-exchange current approach. *Phys Rev D*. 2016;94(9):093004. <https://doi.org/10.1103/PhysRevD.94.093004>. [arXiv:1607.08565](https://arxiv.org/abs/1607.08565). [nucl-th].
  35. Bodek A, Avvakumov S, Bradford R, Budd HS. Vector and Axial Nucleon Form Factors: A Duality Constrained Parameterization. *Eur Phys J C*. 2008;53:349–354. <https://doi.org/10.1140/epjc/s10052-007-0491-4>. [arXiv:0708.1946](https://arxiv.org/abs/0708.1946). [hep-ex].
  36. Bradford R, Bodek A, Budd HS, Arrington J. A New parameterization of the nucleon elastic form-factors. *Nucl Phys B Proc Suppl*. 2006;159:127–132. <https://doi.org/10.1016/j.nuclphysbps.2006.08.028>. [arXiv:hep-ex/0602017](https://arxiv.org/abs/hep-ex/0602017).
  37. Alvarez-Ruso L, Andreopoulos C, Ashkenazi A, Barry C, et al. Recent highlights from GENIE v3. *The European Physical Journal Special Topics*. 2021;p. 1–19.
  38. Metropolis N, Bivins R, Storm M, Turkevich A, Miller JM, Friedlander G. Monte Carlo Calculations on Intranuclear Cascades. I. Low-Energy Studies. *Phys Rev*. 1958;110(1):185. <https://doi.org/10.1103/PhysRev.110.185>.
  39. Katori T. Meson Exchange Current (MEC) Models in Neutrino Interaction Generators. *AIP Conf Proc*. 2015;1663(1):030001. <https://doi.org/10.1063/1.4919465>. [arXiv:1304.6014](https://arxiv.org/abs/1304.6014). [nucl-th].
  40. Bodek A, Budd HS, Christy ME. Neutrino Quasielastic Scattering on Nuclear Targets: Parametrizing Transverse Enhancement (Meson Exchange Currents). *Eur Phys J C*. 2011;71:1726. <https://doi.org/10.1140/epjc/s10052-011-1726-y>. [arXiv:1106.0340](https://arxiv.org/abs/1106.0340). [hep-ph].
  41. Berger C, Sehgal LM. Lepton mass effects in single pion production by neutrinos. *Phys Rev D*. 2007;76:113004. <https://doi.org/10.1103/PhysRevD.76.113004>. [arXiv:0709.4378](https://arxiv.org/abs/0709.4378). [hep-ph].
  42. Rein D, Sehgal LM. Neutrino Excitation of Baryon Resonances and Single Pion Production. *Annals Phys*. 1981;133:79–153. [https://doi.org/10.1016/0003-4916\(81\)90242-6](https://doi.org/10.1016/0003-4916(81)90242-6).
  43. Hernandez E, Nieves J, Valverde M. Neutrino induced weak pion production off the nucleon. *Mod Phys Lett A*. 2008;23:2317–2320. <https://doi.org/10.1142/S0217732308029289>. [arXiv:0802.1627](https://arxiv.org/abs/0802.1627). [hep-ph].
  44. Kuzmin KS, Lyubushkin VV, Naumov VA. Lepton polarization in neutrino nucleon interactions. *Mod Phys Lett A*. 2004;19:2815–2829. <https://doi.org/10.1142/S0217732304016172>. [arXiv:hep-ph/0312107](https://arxiv.org/abs/hep-ph/0312107).
  45. Bodek A, Yang UK. Modeling deep inelastic cross-sections in the few GeV region. *Nucl Phys B Proc Suppl*. 2002;112:70–76. [https://doi.org/10.1016/S0920-5632\(02\)01755-3](https://doi.org/10.1016/S0920-5632(02)01755-3). [arXiv:hep-ex/0203009](https://arxiv.org/abs/hep-ex/0203009).
  46. Sjostrand T, Mrenna S, Skands PZ. PYTHIA 6.4 Physics and Manual. *JHEP*. 2006;05:026. <https://doi.org/10.1088/1126-6708/2006/05/026>. [arXiv:hep-ph/0603175](https://arxiv.org/abs/hep-ph/0603175).
  47. Koba Z, Nielsen HB, Olesen P. Scaling of multiplicity distributions in high-energy hadron collisions. *Nucl Phys B*. 1972;40:317–334. [https://doi.org/10.1016/0550-3213\(72\)90551-2](https://doi.org/10.1016/0550-3213(72)90551-2).
  48. Duffy K. High-Pressure Gaseous Argon TPC for the DUNE Near Detector. In: Meeting of the Division of Particles and Fields of the American Physical Society; 2019. .
  49. Abi B, et al. Experiment Simulation Configurations Approximating DUNE TDR. 2021 3;[arXiv:2103.04797](https://arxiv.org/abs/2103.04797). [hep-ex].
  50. Fleming B. The MicroBooNE Technical Design Report. 2012 2;<https://doi.org/10.2172/1333130>.
  51. Hewes V, et al. Deep Underground Neutrino Experiment (DUNE) Near Detector Conceptual Design Report. *Instruments*. 2021;5(4):31. <https://doi.org/10.3390/instruments5040031>. [arXiv:2103.13910](https://arxiv.org/abs/2103.13910). [physics.ins-det].
  52. Hamacher-Baumann P, Lu X, Martín-Albo J. Neutrino-hydrogen interactions with a high-pressure time projection chamber. *Phys Rev D*. 2020;102(3):033005. <https://doi.org/10.1103/PhysRevD.102.033005>.



- 
- [arXiv:2005.05252](https://arxiv.org/abs/2005.05252). [physics.ins-det].
53. Singh J, Nagu S, Singh J, Singh RB. Quantifying multi-nucleon effect in Argon using high-pressure TPC. *Nucl Phys B*. 2020;957:115103. <https://doi.org/10.1016/j.nuclphysb.2020.115103>. [arXiv:1909.10329](https://arxiv.org/abs/1909.10329). [nucl-th].
54. Coloma P, Huber P. Impact of nuclear effects on the extraction of neutrino oscillation parameters. *Phys Rev Lett*. 2013;111(22):221802. <https://doi.org/10.1103/PhysRevLett.111.221802>. [arXiv:1307.1243](https://arxiv.org/abs/1307.1243). [hep-ph].
55. Adams C, et al. The Long-Baseline Neutrino Experiment: Exploring Fundamental Symmetries of the Universe. In: *Snowmass 2013: Workshop on Energy Frontier*; 2013. .